Dissociative chemisorption of H on Cu(100): A four-dimensional study of the effect of parallel translational motion on the reaction dynamics.

Kroes, G.J.; Wiesenekker, G.; Baerends, E.J.; Mowrey, R.C.; Neuhauser, D.

published in
Journal of Chemical Physics
1996

DOI (link to publisher)
10.1063/1.472450

document version
Publisher's PDF, also known as Version of record

Avoiding long propagation times in wave packet calculations on scattering with resonances: A hybrid approach involving the Lanczos method

Geert-Jan Kroes
Theoretische Chemie, Vrije Universiteit, De Boelelaan 1083, 1081 HV Amsterdam, The Netherlands

Daniel Neuhauser
Department of Chemistry and Biochemistry, University of California, 405 Hilgard Avenue, Los Angeles, California 90095

(Received 13 May 1996; accepted 23 August 1996)

We investigate the usefulness of a hybrid method for scattering with resonances. Wave packet propagation is used to obtain the time-dependent wave function $\Psi(t)$ up to some time T at which direct scattering is over. Next, $\Psi(t)$ is extrapolated beyond T employing resonance eigenvalues and eigenfunctions obtained in a Lanczos procedure, using $\Psi(T)$ as starting vector to achieve faster convergence. The method is tested on one two-dimensional (2D) and one four-dimensional (4D) reactive scattering problem, affected by resonances of widths 0.1–5 meV. Compared to long time wave packet propagation, the hybrid method allows large reductions in the number of Hamiltonian operations N_H required for obtaining converged reaction probabilities: A reduction factor of 24 was achieved for the 2D problem, and a factor of 6 for the 4D problem. © *1996 American Institute of Physics.* [S0021-9606(96)02344-6]

I. INTRODUCTION

The wave packet method constitutes a very efficient approach to the study of scattering, especially if results are sought for scattering from a single initial state over a range of energies. The approach benefitted from the development of appropriate grid representations,[1,2] propagation methods,[3,4] spectral analysis techniques,[5] and methods aimed at restricting the wave function to the physically important region of the potential energy surface.[5–7] Together, these methods enabled very large-scale calculations on inelastic and reactive scattering.[8–11]

Although the wave packet method is very successful, a bottleneck may arise if the scattering is affected by the temporary population of metastable states (''resonances'').[12–14] This is obvious for a time-dependent (TD) formalism: If the resonances have a long lifetime, a long propagation time will be required for allowing the resonances to ''leak away'' to the asymptotic region(s). Perhaps surprisingly, time-independent (TI) implementations similarly experience convergence problems in the presence of resonances.[15,16]

A recently proposed solution[5] to the resonance problem follows naturally if the scattering is considered from the time-dependent point of view. Direct scattering will be over after a relatively short period of time, say T. A natural strategy then consists in adopting the TD formalism in a two-step procedure. In the first step, a suitably chosen initial wave function $\Psi(t=0)$ is propagated directly to $t=T$. During this first step, a transition is enforced from scattering boundary conditions (valid at $t=0$) to fully absorbing boundary conditions (valid at $t=T$). For $t>T$, it is then justified to continue $\Psi(t)$ in time analytically by using an expansion in terms of resonance eigenfunctions Φ_n

$$\Psi(t)=\sum_n d_n \exp[(-i\epsilon_n-\Gamma_n/2)(t-T)]\Phi_n. \qquad (1)$$

The second step of the calculation then consists in computing the energies ϵ_n, widths Γ_n, and weight factors d_n of the resonances, where $d_n=(\Phi_n|\Psi(T))$. Here, $(\Phi_n|\Psi(T))$ defines a type of inner product which differs from the usual Hermitean inner product, as is discussed in Sec. II B. Scattering results will be obtained through the use of time-to-energy Fourier transforms (see below), and, integrating from $t=0$ to infinity the whole procedure is equivalent to a TI scattering method. The only reason the TD formalism is resorted to is that it enables one to introduce a parameter (T) which allows the problem to be partioned in an efficient way.

Implementations of the method described above may differ in the way $\Psi(T)$ is calculated and in the method used to compute ϵ_n, Γ_n, Φ_n, and d_n. In the first implementation,[5] resonance energies, widths, and wave functions were obtained using filter diagonalization (FDG).[5,17–24] The method was applied to the collinear $H+H_2$ reaction on the LSTH surface.[25] Even though this system only displays broad resonances ($\Gamma\approx 10$ meV or more for most resonances) and resonance wave functions were generated in a separate wave packet calculation, the total propagation time required for obtaining converged reaction probabilities was halved when applying the hybrid strategy described above. In the same work, the use of a Lanczos method[26] to obtain resonance eigenvalues and eigenfunctions was mentioned as a viable alternative to filter diagonalization for cases where only a few narrow resonances affect the scattering.

Here, we investigate the performance of a Lanczos procedure for describing the resonance decay in the framework of a scattering calculation. At this point, a comparison with other methods[5,17–24,27,28] will not be made. The purpose of the present work is limited to showing that, compared to ''brute-force'' long-time wave packet propagation, the use of Lanczos to extrapolate $\Psi(T)$ can result in significant computational savings also for a fairly large scattering problem (see below).

The Lanczos method was first used to compute resonance eigenvalues by Milfeld and Moiseyev.[29] Because we use the method here in the context of a scattering calculation requiring the description of the resonance decay described in Eq. (1), in the present application we also use the Lanczos method to obtain resonance eigenfunctions which are used to obtain the expansion coefficients in Eq. (1) and to obtain the overlap of the eigenfunctions with asymptotic states required to obtain scattering information (see also Sec. II B).

The wave packet method is particularly efficient at generating results for scattering from one initial state. At the same time, it is known that the Lanczos algorithm converges specific eigenvalues more quickly if the vector used to start the Lanczos recursion significantly overlaps the corresponding eigenvectors (''guided Lanczos'').[29–32] The above two considerations lead to an obvious choice of starting vector: For a single initial state calculation, one should select $\Psi(T)$, because it significantly overlaps the resonance states of interest [see Eq. (1)] and because it is available at no extra cost from the first part of the calculation. This is the scheme we use here. In applications where results are wanted for quite a few initial states, it may be more efficient to compute resonances in one separate calculation and use the results to extrapolate the wave function for the scattering of all different initial states; this scheme is not pursued here.

A procedure which may lead to a reduction in the number of Lanczos iterations required for converging specific eigenvalues is to use a ''spectral transform'' $f(\hat{H})$ of the Hamiltonian $\hat{H}$ rather than $\hat{H}$ itself in the Lanczos recursion.[27,32–36] Whether such an approach is more efficient (requires less Hamiltonian operations) depends on how many Hamiltonian operations are required to evaluate the action of $f(\hat{H})$ on a Lanczos vector. Because experience with respect to this issue is mixed,[32,36] in the present work we simply use $\hat{H}$.

Of course, other scattering methods which are based on Lanczos recursions[37–40] have already been developed. One example is the recursive residue generation method (RRGM).[37] The use of this method is less appropriate if results are sought for scattering from only one (or a few) initial state(s), as the calculation of a single column of the S matrix requires Lanczos recursions for the initial and all final states. A Lanczos-based method which is more appropriate for this purpose is the recently developed quasiminimal residual (QMR) method.[38,39] While a comparison of the performance of this algorithm and our method should be of interest, it is not attempted in the present work.

Here, the performance of the Lanczos extrapolation procedure is tested for a small (two-dimensional, 2D) and a fairly large (four-dimensional, 4D) problem representing the reactive scattering of H_2 by Cu(100), for which density functional potential energy surfaces have recently become available in analytical form.[41] In this system, the population of Feshbach-type resonance states can occur through vibrational excitation of the molecular bond which becomes weakened at the surface.[42] The 4D problem is fairly difficult, with both narrow and broad resonances, the broad resonances overlapping to some extent. The Hamiltonians for these systems and details of the scattering and extrapolation method are presented in Sec. II. In this section, special attention is given to the problem of how to optimally impose absorbing boundary conditions using optical potentials, i.e., by making the optical potential channel dependent. Results of using the Lanczos procedure to extrapolate $\Psi(T)$ are compared with results of long time wave packet calculations in Sec. III. Sec. IV gives conclusions.

II. METHOD

In this section we describe how to apply the guided Lanczos method to molecule-surface scattering with resonances. General aspects of the time-dependent wave packet method for molecule-surface scattering are presented in Sec. II A. Most of Sec. II A also applies to gas phase scattering, if the molecule-surface distance Z is replaced by the intermolecular distance R. In Sec. II B, we specialize to a description of scattering with resonances, also providing details of the Lanczos method used. Section II C presents the Hamiltonians used in the present work. In Sec. II D, we discuss how the transition from scattering boundary conditions to full absorbing boundary conditions is enforced with the use of an optical potential, also giving some consideration to the form of optical potential employed. Section II E gives computational details.

A. TD wave packet theory for molecule-surface scattering

For scattering of a molecule in an initial state j at total energy E, the scattering boundary condition may be written

$$\Psi_j^+(E|Z_\infty,s)=\frac{\exp[-ikZ_\infty]}{\sqrt{2\pi}}\,\phi_j(s)-\sum_{j'}\left(\frac{k}{k_{j'}}\right)^{1/2}\times\frac{\exp[+ik_{j'}Z_\infty]}{\sqrt{2\pi}}\,\phi_{j'}(s)S_{j'j}(E). \tag{2}$$

In Eq. (2), Z_∞ is an asymptotic value of the scattering coordinate, s is the vector of all other coordinates, and $\Psi_j^+(E|Z_\infty,s)$ is the stationary wave function describing scattering from an initial molecular state j [described by $\phi_j(s)$] at $E=k^2/2M+E_j$, M being the mass of the molecule and E_j being its initial internal energy. Furthermore, $k_{j'}$ is the momentum of a scattered molecule of final state j'. The probability for scattering to the final state j' is related to the S-matrix element $S_{j'j}(E)$ through $P_{j'j}(E)=|S_{j'j}(E)|^2$. To obtain the stationary wave function $\Psi^+(E)$, we set up an initial wave function $\Psi_j(0)$ which moves to the left and which has nonnegligible amplitude only in the region $Z_\infty<Z<Z_{\max}$ using

$$\Psi_j(0)=\phi_j(s)\int_{-\infty}^{\infty}dk'b(k')\,\frac{\exp(ik'Z)}{\sqrt{2\pi}}, \tag{3}$$

where $b(k)$ is chosen to describe a Gaussian wave packet of width ζ which is initially centered on Z_0 and moves toward the surface with an average (negative) momentum k_{av}

$$b(k)=\left(\frac{2\xi^2}{\pi}\right)^{1/4}\exp[-(k_{\mathrm{av}}-k)^2\xi^2]+i(k_{\mathrm{av}}-k)Z_0]. \quad (4)$$

In the version of the time-dependent (TD) method we employ, one acts with the evolution operator $\hat{U}(t)$ on $\Psi_j(0)$ to obtain $\Psi_j(t|Z_\infty)$, propagating the wave function in and out of the interaction region and saving the overlaps

$$C_{j'j}(t,Z_\infty)=\int ds\,\phi_{j'}(s)^*\Psi_j(t|Z_\infty) \quad (5)$$

of $\Psi_j(t|Z_\infty)$ with asymptotic states $\phi_{j'}(s)$. One could then obtain the stationary wave function at Z_∞ through a time-to-energy Fourier transform.[10] Here, we use fast Fourier transforms to obtain energy-dependent overlaps $A_{j'}j(E,Z_\infty)$ on a grid of energies using

$$A_{j'j}(E,Z_\infty)=\int_{t=0}^{\infty} dt\,\exp(iEt)C_{j'j}(t,Z_\infty). \quad (6)$$

In case the $A_{j'j}(E,Z_\infty)$ are also required at intermediate energies, they can be obtained using interpolation. In practical cases, the limit $t=\infty$ in Eq. (6) is replaced by some time T at which the wave function is supposed to have left the asymptotic region. This will not suffice in case resonances are important; the way in which Eq. (6) is modified to deal with the resonance case is discussed below in Sec. II B.

From the $A_{j'j}$, S-matrix elements may be obtained using[43,44]

$$S_{j'j}(E)=\delta_{j'j}\exp[-2ikZ_\infty] - \sqrt{\frac{kk_{j'}}{2\pi}}\frac{\exp[-ik_{j'}Z_\infty]}{Mb(-k)}A_{j'j}(E,Z_\infty). \quad (7)$$

B. Specialization to resonances: Application of the Lanczos method

In case resonances occur, the total propagation time T that would be required to converge the overlap integral of Eq. (6) with $t=\infty$ replaced by $t=T$ may become forbiddingly large. As suggested by Eq. (1), we partition the integral in Eq. (6) as

$$A_{j'j}(E,Z_\infty)=\int_{t=0}^{T} dt\,\exp(iEt)C_{j'j}(t,Z_\infty) + \int_{t=T}^{\infty} dt\,\exp(iEt)C_{j'j}(t,Z_\infty). \quad (8)$$

We define

$$A_{j'j}(E,Z_\infty;T)=\int_{t=0}^{T} dt\,\exp(iEt)C_{j'j}(t,Z_\infty) \quad (9)$$

and

$$C_{j'n}(Z_\infty)=\int ds\,\phi_{j'}(s)^*\Phi_n(Z_\infty,s). \quad (10)$$

For $t>T$, we have [substituting $\Psi(t)$ of Eq. (1) for $\Psi_j(t|Z_\infty)$ in Eq. (5)]

$$C_{j'j}(t,Z_\infty)=\sum_n C_{j'n}(Z_\infty)d_n\exp[(-i\epsilon_n-\Gamma_n/2)(t-T)]. \quad (11)$$

Substituting Eq. 11 into the second integral of Eq. 8, analytical evaluation yields

$$A_{j'j}(E,Z_\infty)=A_{j'j}(E,Z_\infty;T)+\exp(iET) \times\sum_n d_nC_{j'n}(Z_\infty)\frac{1}{i(\epsilon_n-E)+\Gamma_n/2}. \quad (12)$$

Equation (12) shows that in order to get all scattering information [Eq. (7)], we require in addition to the $C_{j'j}(t,Z_\infty)$ for $t<T$ the energies ϵ_n, widths Γ_n, and weights d_n of the resonances that make large contributions to $\Psi(T)$. In addition, we need the resonance wave functions Φ_n on the cut $Z=Z_\infty$ [Eq. (10)], but we do not require the full resonance wave functions to be available. This will be especially advantageous if much storage would be required for the Φ_n. On the other hand, having the Φ_n available can be useful for analyzing how the resonances affect the scattering.

Of course, the idea expressed by Eq. (1) (describing the resonance decay analytically) can also be implemented using different methods of asymptotic analysis, such as the T-matrix formalism[45] used in the original application of the hybrid method,[5] or flux analysis methods which allow the use of smaller values for Z_∞.[46]

Resonance eigenvalues and eigenvectors are obtained by an implementation of the Lanczos method for complex symmetric matrices due to Cullum and Willoughby.[47] As discussed in their book (see also Ref. 29), the major difference between the Lanczos method for complex symmetric matrices and the method for Hermitian matrices is that a different type of inner product (called ''Euclidean inner product'' by Cullum and Willoughby[47]) has to be used for obtaining the elements of the Lanczos tridiagonal matrix. The Euclidean inner product of two functions ϕ and ψ is defined as

$$(\phi|\psi)\equiv\langle\phi^*|\psi\rangle=\int \phi(\tau)\psi(\tau)\,d\tau,$$

so that $(\phi|\psi)=(\psi|\phi)$. With the inner product defined as above, complex symmetric Hamiltonian matrices are obtained by adding an optical potential to the Hamiltonians discussed in Sec. II C, and by representing the resulting Hamiltonian and the wave functions ϕ and ψ in a set of real basis functions. With the use of real basis functions, the Euclidean inner product is equal to the c-product defined by Moiseyev *et al.*,[48] although it should be noted that the c-product has a more general definition allowing its use also with complex basis functions[49] (this is not relevant for the present application, in which we require the Hamiltonian matrix to be complex symmetric). It should be noted that, if real basis functions are used, a complex symmetric Hamiltonian can also be obtained with the use of a complex scaling approach;[50,51] this approach was used in the first application of the Lanczos method to the calculation of resonances.[29]

Rather then reorthogonalizing the generated Lanczos vectors with respect to one another, the implementation by Cullum and Willoughby[47] uses an algorithm to identify spurious eigenvalues arising from the loss of orthogonality. For our purpose, resonance eigenvectors also need to be obtained: Due to loss of orthogonality, the weights can only be obtained from $d_n=(\Phi_n|\Psi(T))$ by computing the eigenvectors Φ_n and normalizing them. Eigenvectors are calculated as described in Ref. 47, by first computing the Lanczos vectors using inverse iteration and then repeating the Lanczos recursion to obtain the so-called Ritz vectors (the Lanczos approximations to the resonance eigenvectors). We note that methods based on Lanczos recursion and not requiring eigenvectors exist for the calculation of transition probabilities;[37,52] however, in the sum of Eq. (12) [or, alternatively, Eq. (1)] we require the ''transition amplitude'' d_n, i.e., we also need to know its phase.

The eigenvalues for which H eigenvectors are obtained are selected on the basis of convergence with number of Lanczos iterations. The accuracy of the Φ_n can be judged by computing the error norm $\|(\hat{H}-\epsilon_n\hat{I})\Phi_n\|$.

We note that, for optimal efficiency, a method should be available for estimating the value of T for which the hybrid method is most efficient computationally. In the present work, the approach was to try some value of T and check whether converged results could be obtained with the use of a reasonable number of Lanczos iterations; otherwise T was increased until convergence was achieved. Efforts aimed at fine-tuning the method will be made in future work, where we compare the efficiency of the present implementation of the hybrid method (using Lanczos) with that of other implementations (for instance, using filter diagonalization[5,17–19]).

C. Hamiltonians

The 2D problem we solve is representative of the reaction of H_2 colliding with a top site of the (100) face of Cu. The molecular axis is kept parallel to the surface, the atoms dissociating to bridge sites. The Hamiltonian is written (using atomic units)

$$\hat{H}_{2D}=-\frac{1}{2M}\frac{\partial^2}{\partial Z^2}-\frac{1}{2\mu}\frac{\partial^2}{\partial r^2}+V_{tb}(r,Z), \tag{13}$$

where r is the H-H distance, M is the mass of the molecule, and μ its reduced mass. In Eq. (13), $V_{tb}(r,Z)$ is the potential energy surface (PES) for dissociation above the top site, the atoms moving to the bridge site. A fully analytical expression for the PES and its parameters are given in Ref. 41.

To solve the 2D Schrödinger equation, the wave function is expanded on a grid of N_Z points with equal spacing in Z and a grid of N_r points with equal spacing in r. The initial wave function is taken as the product of a Gaussian wave packet in Z with the $v=0$ vibrational wave function $\phi_0(r)$ for H_2 [Eqs. (3) and (4)]. Probabilities for vibrationally elastic and inelastic scattering $P_{v'v}(E)$ are obtained from the S-matrix elements [Eq. (7)] using

$$P_{v'v}(E)=|S_{v'v}(E)|^2 \tag{14}$$

and reaction probabilities are obtained by summing the probabilities $P_{v'v}(E)$ over v' and subtracting from one.

In the 4D problem we solve, we still keep the molecular axis parallel to the surface, but now also allow motion of the molecule along the surface (in X and Y):

$$\hat{H}_{4D}=-\frac{1}{2M}\left(\frac{\partial^2}{\partial Z^2}+\frac{\partial^2}{\partial X^2}+\frac{\partial^2}{\partial Y^2}\right)-\frac{1}{2\mu}\frac{\partial^2}{\partial r^2}+V_{4D}(r,Z,X,Y). \tag{15}$$

Once again, a fully analytical expression for the 4D PES is used, the form and parameters of which are given in Ref. 41.

In the present 4D problem, we consider normal incidence only. The wave function is expanded on a grid of points in r and Z and in symmetry adapted functions $H_{nm}(X,Y)$[53,54]

$$\Psi(t)=\sum_{nm} f_{nm}(r,Z,t)H_{nm}(x,y). \tag{16}$$

In Eq. (16), n and m are diffraction quantum numbers. The initial wave function is taken as the product of $\phi_0(r)$ $H_{00}(x,y)$ with a Gaussian wave packet in Z [Eq. (3) and (4)]. Probabilities for diffractionally and vibrationally inelastic scattering $P_{v'nmv}(E)$ are obtained from S-matrix elements $S_{v'nmv}(E)$ as in Eq. (14). Reaction probabilities are obtained by summing the $P_{v'nmv}(E)s$ over v', n, and m, and subtracting from one.

D. Absorbing boundary conditions

In order to compute resonances, fully outgoing boundary conditions need to be imposed. At the same time, in wave packet calculations we usually seek results for a wide range of energies, over which many resonances may affect the scattering. Then, we would like to use a method for imposing absorbing boundary conditions which (i) is stable (results not too dependent on parameters), (ii) can be implemented with the specification of just a few parameters, and yet (iii) yields reasonably accurate eigenvalues when used in resonance calculations, in analogy to complex scaling results (Refs. 50, 51, see especially the work of Moiseyev and his co-workers[52]). Work which compares the performance of optical potentials with that of more formal approaches[55–58] shows that optical potentials meet the above requirements, provided that (i) the parameters are chosen to ensure minimum reflection from and transmission through the optical potentials, and (ii) artificial resonances, which result from reflection or transmission, are identified. A method which provides a good choice of parameters and ensures low contributions of artificial resonances is discussed below; first, we discuss how to effect a transition from scattering to resonance boundary conditions.

To solve the scattering with resonances problem, we have to start out with scattering boundary conditions, and, prior to the calculation of resonances, effect of a transition to fully absorbing boundary conditions in a way that leaves the accuracy of our solution to the scattering problem intact.

This is done in essentially the same way as in the original implementation,[5] with the use of a projection operator formalism.[6,7] At the start of the calculation, we keep the wave function on two grids, writing

$$\Psi(t)=\hat{P}\Psi(t)+(1-\hat{P})\Psi(t). \tag{17}$$

Here, $\hat{P}\Psi(t)$ contains the initial channel on a 1D grid with somewhat larger extent in Z. The part $(1-\hat{P})\Psi(t)$ is kept on a 2D grid with smaller extent in Z. On $(1-\hat{P})\Psi(t)$, fully absorbing boundary conditions are imposed from the start using optical potentials V_I which pad the asymptotic reactants and products regions (starting at $Z=Z_{\min}^{\mathrm{opt}}=Z_\infty$ and $r=r_{\min}^{\mathrm{opt}}$, respectively). In the present implementation,[44] fully absorbing boundary conditions are imposed by adding $\hat{P}\Psi(t)$ to $(1-\hat{P})\Psi(t)$ and continuing propagation on one (2D) grid, once $\hat{P}\Psi(t)$ can be fully accommodated on the 2D grid within the optical potentials padding it. At this point, fully absorbing boundary conditions are imposed.

In both the reactants and products region, we employ a quadratic negative imaginary potential

$$V_I(\overline{x})=-i\,\tfrac{3}{2}\,A_2\overline{x^2}, \tag{18}$$

where

$$\overline{x}=(Z-Z_{\min}^{\mathrm{opt}})/L_Z, \quad \text{reactants}, \tag{19}$$

$$\overline{x}=(r-r_{\min}^{\mathrm{opt}})/L_r, \quad \text{products}. \tag{20}$$

In Eqs. (19) and (20), $Z_{\min}^{\mathrm{opt}}$ ($r_{\min}^{\mathrm{opt}}$) defines the initial value of the coordinate $Z(r)$ at which V_I starts to act, and $L_Z(L_r)$ defines its range. Optimal values for the A_2 parameter can be calculated from the average energy with which the wave packet is expected to emerge through linear interpolation of Table III of Ref. 59. The choice of A_2 may become critical if the wavelength associated with the motion by which the fragments separate becomes comparable to the range L of V_I.[59] For this reason we employ a channel-dependent V_I in the reactants zone. Rather than specifying A_2 directly, we specify $E_{\mathrm{aim}}^{\mathrm{opt}}$ and for each channel calculate A_2^{ch} from the translational energy

$$E_{\mathrm{ch}}=E_{\mathrm{aim}}^{\mathrm{opt}}-(E_{\mathrm{ch}}^{\mathrm{int}}-E_0^{\mathrm{int}}) \tag{21}$$

using linear interpolation of Table III of Ref. 59. In Eq. (21), E_0^{int} is the internal energy associated with the initial internal states of the scattering particles, and $E_{\mathrm{ch}}^{\mathrm{int}}$ is the internal energy associated with the final channel. One way to chose $E_{\mathrm{aim}}^{\mathrm{opt}}$ would be to set it to the average translational energy of the initial wave packet; recognizing that the choice of A_2 is more critical at low translational energies, we usually set it to a somewhat lower value. A second parameter $E_{\mathrm{ch}}^{\min}$ specifies that the A_2^{ch} value appropriate for a translational energy equal to $E_{\mathrm{ch}}^{\min}$ should be selected if E_{ch} should be less than $E_{\mathrm{ch}}^{\min}$.

Because the reaction studied is slightly exothermic, the products are expected to emerge from the barrier with much energy in the H-H motion, with a small associated wavelength. Therefore, the choice of A_2 is less critical in the products region, and we take it channel independent.

TABLE I. Values of input parameters to the 2D and 4D reactive scattering calculations. Unless indicated otherwise, parameters are in atomic units.

Parameter	2D	4D
$r_{\min}$ (minimum value r on grid)	0.522	0.522
Δr (grid spacing in r)	0.15	0.15
N_r (number of grid points in r)	48	48
$Z_{\min}$ (minimum value Z on grid)	−1.0	−1.0
ΔZ (grid spacing in Z)	0.15	0.15
N_Z (number of grid points in Z)	120	120
N_P (number of grid points in Z, 1D grid)	160	160
Z_∞ (analysis value of Z)	12.05	12.05
L_Z (range of optical potential in Z)	4.0	4.0
$Z_{\min}^{\mathrm{opt}}$ (starting point of optical potential V_I)	12.05	12.05
$E_{\mathrm{aim}}^{\mathrm{opt}}$ (collision energy for which V_I is optimal, eV)	0.25	0.25
$E_{\mathrm{ch}}^{\min}$ (see Sec. II D, eV)	0.03	0.03
$r_{\min}^{\mathrm{opt}}$ (starting point of optical potential V_I)	4.822	4.822
L_r (range of optical potential in r)	2.0	2.0
A_2 (parameter for optical potential in r)	0.045	0.045
ζ (width initial wave packet)	0.3718	0.3718
k_{av} (average momentum initial wave packet)	−10.04	−10.04
Z_0 (average Z value of initial wave packet)	14.0	14.0
Δt (timestep, fs)	2.42	1.45
T_l (total propagation time, ps)	19.36	15.68
T_{cut} (see text, eV)	5.5	5.5
V_{cut} (see text, eV)	5.5	none
O_d (maximum diffraction order $\lvert n\rvert+\lvert m\rvert$)	0	12
N_{XY} (number of basis functions in X and Y)	1	49

E. Numerical details

Input parameters to the 2D and 4D wave packet calculations are collected in Table I. The wave function is propagated in time using the Chebyshev method[3] using a timestep Δt (see Table I). To increase the efficiency of the Chebyshev algorithm, a cutoff value T_{cut} was imposed on the kinetic energy operator, and, in the 2D problem, a cutoff value V_{cut} is imposed on the potential (see Table I). In the 4D problem, the maximum value of V is 1 hartree. Cutoff values employed in the time propagation are likewise employed in the subsequent resonance calculations using Lanczos.

The size of the basis set effectively used in the 2D problem is $N_Z\times N_r=5760$, and the size of the basis set in the 4D problem is $N_Z\times N_r\times N_{XY}=282\,240$. While the 2D problem is ''small,'' the 4D problem is moderately large even by modern standards. In both calculations, the initial state of H_2 is the vibrational ($v=0$) ground state. Computational details concerning the Lanczos computation of resonances will be given in the next section.

III. RESULTS AND DISCUSSION

A. The 2D problem

For the 2D problem, Figs. 1(a) ($T=0.6$ ps) and 1(b) ($T=19.4$ ps) show that long times (>19.4 ps) are necessary for convergence in the direct propagation. The hybrid propagation+Lanczos method uses, in contrast, direct propagation only until a very short time ($T=0.6$ ps). At that time, direct propagation obviously yields a wave function which is still far from being converged [with negative reaction probabilities calculated for some energies, see Fig. 1(a)]. But us-

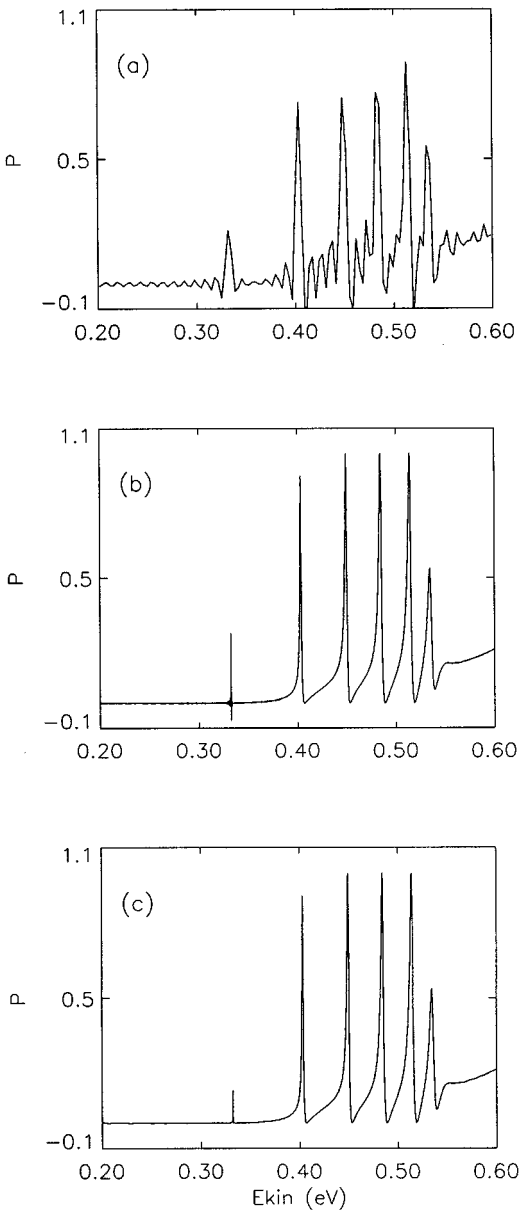

FIG. 1. Reaction probabilities are shown as a function of the collision energy for the 2D problem. The results are for: (a) direct wave packet propagation ($T=0.6$ ps); (b) same, but $T=19.4$ ps; (c) the hybrid method. In (a), the energy resolution is 3.42 meV; in (b) and (c) the energy resolution is 0.107 meV.

ing the hybrid method, this T is sufficient. Specifically, $\Psi(T=0.6$ ps) was taken as the initial vector for a Lancosz recursion, with 2000 vectors. Six resonance eigenvalues and eigenvectors were obtained with energies in the relevant region for the scattering of $v=0$ H_2 at collision energies between 0.2 and 0.6 eV, their widths ranging from 0.2 meV to 4.4 meV (see Table II).

When the short-time direct and the Lancosz components were added [Eq. (12) with $T=0.6$ ps, see Fig. 1(c)], the resulting reaction probabilities are well converged; they agree with the long-time Chebyshev simulation ($T=19.4$ ps) to better than 1% except near the narrow resonance at 0.332 eV, where the disagreement is due to well-known aliasing

TABLE II. Properties of the 2D resonance states. Below, ϵ_n denotes the real part of the energy λ_n of resonance n, Γ_n its width, and R_n the error norm $\|(\hat{H}-\lambda_n I)\phi_n\|$ of the associated eigenvector ϕ_n. For reference, we also give the collision energy $E_c=\epsilon_n-E(v=0)$, where $E(v=0)$ is the energy of H_2 in its vibronic ground state. All results were obtained using 2000 Lanczos iterations.

n	E_c (eV)	ϵ_n (eV)	Γ_n (eV)	R_n (eV)
1	0.332 31	−4.238 00	0.2071(−3)	0.28(−5)
2	0.403 41	−4.166 90	0.1440(−2)	0.44(−6)
3	0.449 70	−4.120 60	0.2151(−2)	0.67(−7)
4	0.484 82	−4.085 49	0.2886(−2)	0.24(−6)
5	0.514 74	−4.055 57	0.3475(−2)	0.12(−4)
6	0.535 59	−4.034 71	0.4441(−2)	0.60(−4)

difficulties[60,61] in the direct simulation, which even at long times is not yet well converged (see Fig. 2). Note that the energy resolution in Fig. 1(c) is the same as that in Fig. 1(b). To achieve the high energy resolution in the hybrid method, the technique of frequency shifting[60,61] was combined with fast Fourier transforms to obtain the $A_{j'j}(E,Z_\infty;T)$ [Eq. (9)] on a denser energy grid.

The number of Hamiltonian operations N_H required in the brute force long-time propagation (19.4 ps) is large (488 000), but is reduced by a factor 24 ($N_H=20\,489$) in the hybrid calculation: 15 250 operations are needed to calculate $\Psi(T=0.6$ ps), 2000 operations to calculate eigenvalues, and 3239 operations are required to obtain eigenvectors (the Cullum and Willoughby algorithm[47,62] employs more iterations in the eigenvector calculation to extract eigenvectors as accurately as possible).

The partitioning of the problem into a calculation of direct scattering and of resonance decay makes the hybrid approach also more efficient than a TI approach in which the coefficients of the Chebyshev sum are integrated analytically over time[63–65] and where convergence is ensured by the use of a modified Chebyshev recursion.[65] This is shown in Fig. 3, where the modified TI approach[65] is shown to perform just

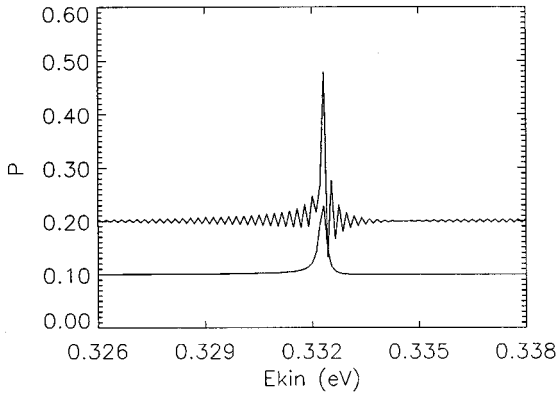

FIG. 2. Reaction probabilities are shown as a function of the collision energy for the 2D problem in the vicinity of a narrow resonance (no. 1 of Table II). The smooth curve was calculated by the hybrid method (results shifted upward by 0.1). The oscillating curve results from direct wave packet propagation with $T=19.4$ ps.

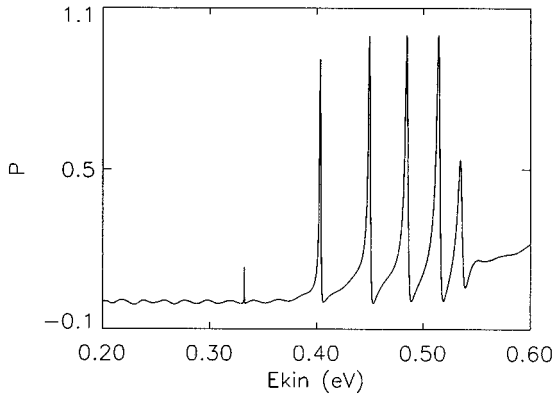

FIG. 3. Reaction probabilities are shown as a function of the collision energy for the 2D problem. The results were obtained using a time-independent wave packet method.[15] The energy resolution is 0.107 meV.

as bad as the brute-force TD approach (for the same number of Hamiltonian operations, 488 000). Apparently, the modified TI approach, which has recently been shown[15] to be typically three times more efficient than a multiple-timestep TD wave packet approach for direct scattering problems, is not as effective here, due to the resonances: The hybrid method, which takes into account the physics of the problem, is much more efficient (by a factor 24). We note that, in the TI approach, more rapid convergence can be enforced with the use of a damping factor; while this procedure enforces faster convergence, it does not produce accurate results near resonances.[16]

Before proceeding to the 4D problem, one point remains to be made concerning the convergence of eigenvalues with the use of the Lanczos algorithm without reorthogonalization.[47,62] In this method, eigenvalues and vectors are best when first converged; their quality detoriates once ''copies'' start to form (this explains why the error norms for resonances 1 and 2 in Table II are larger than the error norms for eigenvalues 3 and 4; eigenvalues 1 and 2 had already formed ''copies''). In the 4D calculations, in the eigenvector calculations we make use of this property of the method by attempting a number of different values N_n^{it} around the number of iterations N_L^n at which eigenvalue λ_n has first converged, instead of around the total number of Lanczos iterations N_L (as is done in the original algorithm[47,62]). To this end, eigenvalue computations were performed also for intermediate values of N_L.

B. The 4D problem

For the 4D problem, Fig. 4 illustrates the differences between direct wave packet results for $T=1.3$ ps and $T=15.7$ ps for collision energies between 0.35 and 0.6 eV. Over this range, the scattering is affected by more than 20 narrow resonances, presenting a real challenge to the extrapolation method. We do not show results for energies less than 0.35 eV; in this range reaction probabilities are small and not affected by resonances.

Next, $\Psi(T=1.3\ \mathrm{ps})$ was used to start a Lanczos recursion, computing eigenvalues for $N_L=1$, 2, 3, 4, 6, 8, 10, 15, 20, and 30×10^3, and monitoring their convergence (this is not done in the Cullum and Willough method[62]). In modeling the resonance decay, all resonances for which the energies were converged to within less than 10^{-4} eV were used in the collision energy range 0.2–0.5 eV. In the range 0.5–0.6 eV, all resonances which were identified as ''good'' by the Cullum and Willoughby algorithm were used. The 26 resonances identified in the range 0.2–0.6 eV (we add one at slightly higher energy affecting the scattering near 0.60 eV) are listed in Table III. The widths of the resonances range from 0.16 meV to 3.7 meV. The deviations Δ_n give the difference between the eigenvalue calculated using the value of N_L^n listed in the table and using the highest lower value of N_L.

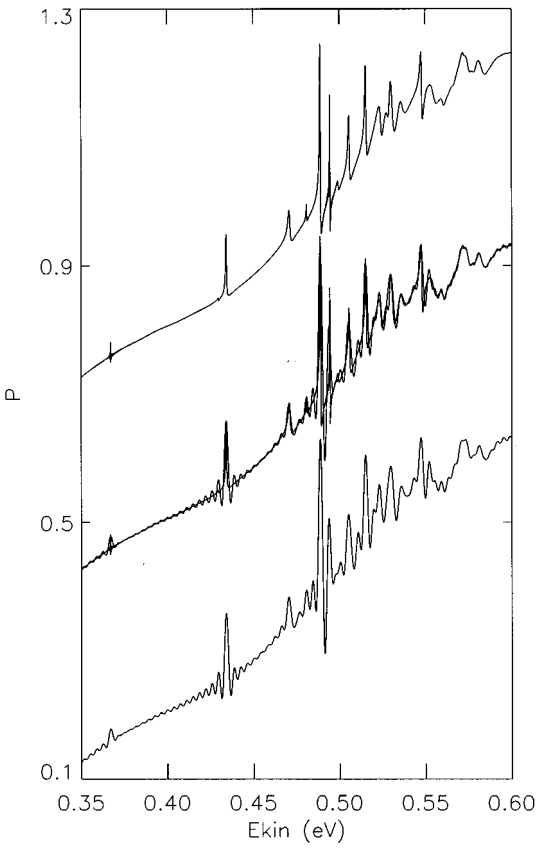

FIG. 4. Reaction probabilities calculated for the 4D problem and resulting from direct wave packet propagation are compared for $T=15.7$ ps (curve shifted upwards by $\Delta P=0.6$) and for $T=1.3$ ps. The energy resolution is 0.132 meV. For a better comparison, both curves are also shown superimposed with a shift of $\Delta P=0.3$.

Adding results of the short time ($T=1.3$ ps) propagation and of the resonance decay [Eq. (12)], converged reaction probabilities are obtained: As shown by Fig. 5, the results of the hybrid method and of long-time propagation ($T=15.7$ ps) agree to within better than 1% except near two narrow resonances occurring at collision energies of 0.367 and 0.494 eV. Plots like Fig. 2, which are not shown here, confirmed that the long-time propagation had not yet converged near these energies, while the hybrid method yields smooth reaction probabilities by modeling the resonance decay correctly.

The better quality of the extrapolated wave packet re-

TABLE III. Properties of the 4D resonance states. Below, ϵ_n denotes the real part of the energy λ_n of resonance n, Γ_n its width, N_L^n the number of Lanczos iterations used to obtain eigenvalue n, Δ_n its estimated convergence, and R_n the error norm $\|(\hat{H}-\lambda_n I)\phi_n\|$ of the associated eigenvector ϕ_n. For reference, we also give the collision energy $E_c=\epsilon_n-E(v=0)$, where $E(v=0)$ is the energy of H_2 in its vibronic ground state.

n	E_c (eV)	ϵ_n (eV)	Γ_n (eV)	N_L	Δ_n (eV)	R_n (eV)
1	0.234 95	−4.335 35	0.2432(−3)	8000	0.2 (−5)	0.94(−2)
2	0.367 05	−4.203 25	0.1574(−3)	6000	0.4(−12)	0.40(−5)
3	0.429 71	−4.140 60	0.3810(−3)	8000	0.5(−10)	0.11(−3)
4	0.434 16	−4.136 14	0.6554(−3)	8000	0.1(−10)	0.65(−5)
5	0.470 97	−4.099 34	0.1418(−2)	8000	0.7(−11)	0.87(−5)
6	0.480 93	−4.089 38	0.3269(−3)	10 000	0.4(−10)	0.50(−5)
7	0.488 92	−4.081 38	0.4941(−3)	8000	0.2 (−9)	0.98(−5)
8	0.494 41	−4.075 90	0.2075(−3)	10 000	0.2 (−9)	0.31(−4)
9	0.499 21	−4.071 09	0.1125(−2)	10 000	0.1 (−7)	0.73(−3)
10	0.505 62	−4.064 69	0.9085(−3)	30 000	0.2 (−8)	0.17(−4)
11	0.505 99	−4.064 32	0.5071(−3)	30 000	>0.1 (−3)	0.11(−1)
12	0.515 38	−4.054 92	0.8204(−3)	30 000	0.1 (−7)	0.65(−3)
13	0.522 76	−4.047 54	0.2157(−2)	30 000	0.2 (−4)	0.14(−1)
14	0.524 07	−4.046 23	0.1961(−2)	30 000	0.8 (−7)	0.12(−2)
15	0.528 79	−4.041 51	0.2160(−2)	30 000	0.1 (−5)	0.96(−3)
16	0.530 40	−4.039 90	0.3395(−2)	30 000	0.1 (−4)	0.81(−2)
17	0.534 41	−4.035 90	0.1497(−2)	30 000	0.1 (−5)	0.21(−2)
18	0.536 62	−4.034 08	0.3721(−2)	30 000	0.1 (−4)	0.61(−2)
19	0.537 72	−4.032 59	0.7627(−3)	30 000	0.3 (−6)	0.13(−2)
20	0.538 19	−4.032 12	0.2421(−2)	30 000	0.8 (−6)	0.39(−2)
21	0.547 84	−4.022 47	0.9658(−3)	30 000	0.5 (−8)	0.98(−5)
22	0.560 34	−4.009 97	0.2541(−2)	30 000	0.3 (−5)	0.18(−2)
23	0.572 50	−3.997 80	0.1766(−2)	30 000	0.8 (−5)	0.61(−3)
24	0.576 96	−3.993 34	0.3391(−2)	20 000	0.1 (−4)	0.91(−1)
25	0.587 96	−3.982 34	0.6677(−3)	30 000	>0.1 (−3)	0.17(−2)
26	0.591 48	−3.978 82	0.1689(−2)	30 000	>0.1 (−3)	0.62(−2)
27	0.603 89	−3.966 44	0.2518(−2)	20 000	0.1 (−7)	0.43(−3)

sults is achieved with much less Hamiltonian operations: the short-time propagation required 72 900 operations, the eigenvalue computation 30 000 operations, and the eigenvector calculation 40 138 operations, yielding $N_H=143\,038$, which is less than the number required in the long-time propagation (874 800) by a factor of 6. Note also that the number of iterations required to converge the most important resonances (30 000) is less than the dimension of the (sparse) full Hamiltonian matrix (282 240) by almost a factor 10.

The 4D resonance calculation was somewhat more difficult than the 2D calculation. First, eigenvalues and eigenvectors are calculated with lower accuracy, due to the greater size of the Hamiltonian matrix, necessitating the use of higher error tolerances in the calculations.[62] Second, because the energy level density is higher in the 4D problem, more iterations are required to produce converged results,[62] especially in the range 0.5–0.6 eV which features many broad resonances. Third, for obtaining convergence with a reasonable number of Lanczos iterations (30 000) it was found necessary to use a some what longer ''short time'' (1.3 ps compared to 0.6 ps for 2D) in the preceding direct propagation run. Fourth, because the energy level density is higher, the algorithm for identifying spurious eigenvalues,[47] which is based on energy differences, sometimes fails, misclassifying ''good'' isolated eigenvalues as ''spurious'' isolated eigenvalues. We found that this can be caught by monitoring the convergence of the eigenvalues: In misclassifications, a converging eigenvalue is seen to disappear. Here, it is helpful that convergence of ''guided'' Lanczos is gradual (as noted also in Ref. 32). Fifth and last, as described below with the use of the hybrid method, the reduction in computation time is not as great as one might infer from the reduction achieved in the number of Hamiltonian operations. While the above problems do not stand in the way of an accurate and efficient computation of reaction probabilities for the present, moderately large system (size basis set=282 240), they may present more serious difficulties for much larger systems.

As can be seen from Table IV, measured in total CPU time the hybrid method is more efficient than the long-time propagation by only a factor 1.7, while six times less Hamiltonian operations were required. The loss of efficiency arises because the diagonalization of the Lanczos tridiagonal complex symmetric matrix (by a QL-type algorithm) is relatively expensive, especially for the present case: The calculations were done on a vector processing machine and, while vector processing is efficient for the other parts of the calculation, the QL algorithm is not vectorizable. In more demanding applications, the diagonalizations could be performed separately on a work station. Weighing the CPU time required by the diagonalizations with a factor 1/10, on a work station the hybrid method should be more efficient by about a factor 3. Note that the diagonalizations could become a computational bottleneck for systems requiring much more iterations, the diagonalization scaling with the number of Lanczos iterations as N_L^2.

The amount of CPU time required for the calculation of

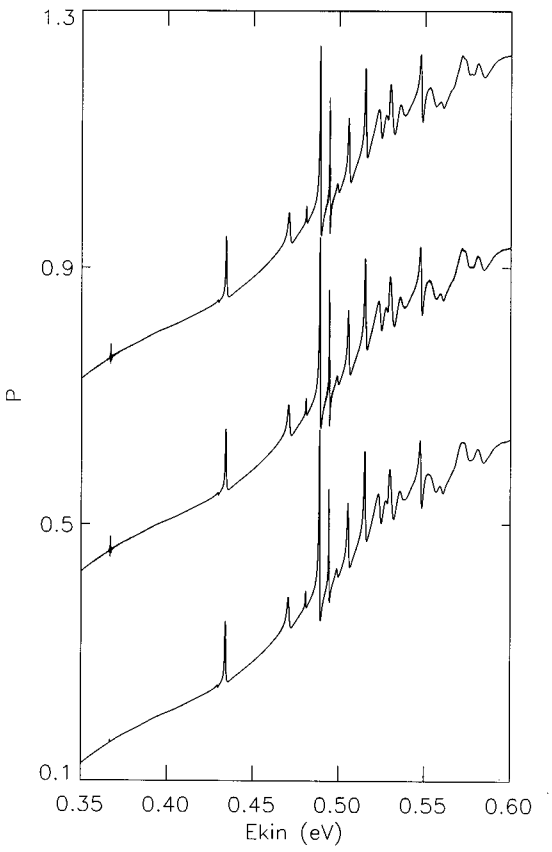

FIG. 5. Reaction probabilities are shown as a function of the collision energy for the 4D problem. The upper curve results from direct wave packet propagation with $T=15.7$ ps (results shifted up by $\Delta P=0.6$). The lower curve shows results of the hybrid method. The energy resolution is 0.132 meV. For a better comparison, both curves are also shown superimposed with a shift of $\Delta P=0.3$.

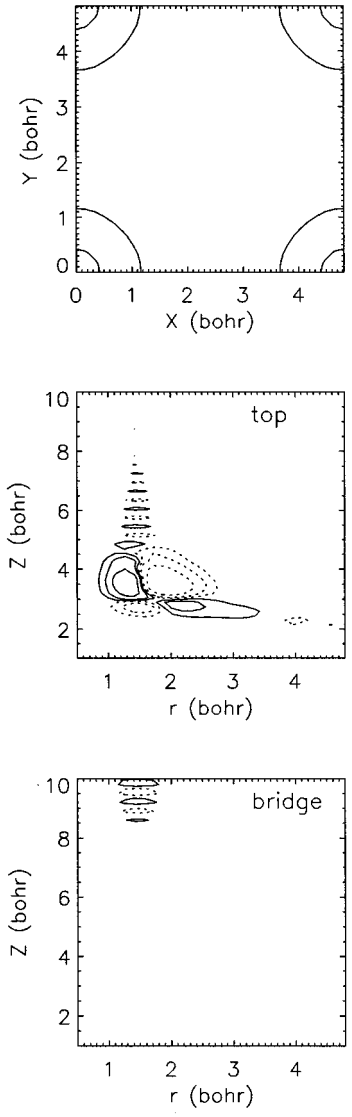

FIG. 6. For resonance 4 of Table III, shown are: (i) a projection of $|\Phi(Z,r,X,Y)|^2$ on the surface unit cell, the top sites being located in the corners, and the bridge sites being located halfway between two neighboring top sites (upper plot); (ii) the functional dependence of $\mathrm{Re}(\Phi)$ on Z and r, above the top site (middle plot); (iii) same, now for the bridge site (lower plot).

TABLE IV. For the 4D reactive scattering problem, CPU times (in seconds) are given for the long time wave packet propagation (A) and the extrapolated wave packet calculation (B). The CPU times listed were obtained on a Cray Y-MP C98.

CPU required for	A	B
$\hat{H}$ operations, wave packet	79 779	6728
Other, wave packet	8451	723
Total, wave packet	88 230	7451
$\hat{H}$ operations, Lanczos eigenvalues	⋯	3058
Lanczos, diagonalizations	⋯	29 965
Lanczos, inverse iterations	⋯	35
Other, eigenvalues	⋯	858
Total, eigenvalues		33 916
$\hat{H}$ operations, Lanczos eigenvectors	⋯	4143
Lanczos, inverse iterations	⋯	22
Lanczos, Ritz vectors	⋯	5648
Other, eigenvectors	⋯	715
Total, eigenvectors	⋯	10 528
Asymptotic analysis	20	23
Total	88 250	51 918

the Ritz vectors is not forbiddingly large (less than 50% of the CPU time required by the extrapolation also if we weight the CPU time required for the diagonalizations). In the present application, the Ritz vectors were kept in direct memory, which took 15 Mw of storage. In more demanding applications, they could be stored on disk using direct access files. The advantage of having eigenvectors available is illustrated in Fig. 6, showing a plot of resonance 4 of Table III. The upper plot shows the wave function to be localized on the top sites of the Cu(100) surface. Above this site, the molecule-surface vibration is excited with one quantum, and the same is true for the molecular bond. In contrast, no quasibound motion is seen above the bridge site. Figure 6 and similar plots presented elsewhere[66] and displaying other resonances of Table III show that the basic mechanism underlying the population of the 4D resonance states is the

same as that seen in 2D calculations for impact on the top sites; in this mechanism, trapping occurs through excitation of the molecular bond which is weakened at the surface, at total energies below the energy of gas phase $v=1$ H_2.

IV. CONCLUDING REMARKS

We have investigated the efficiency of a guided Lanczos procedure in the framework of a hybrid method for scattering with resonances. In this method, the time-independent (TI) scattering problem is solved by efficiently partitioning it into two time-dependent (TD) problems, by introducing the parameter T which denotes a time beyond which the TD wave function can be expanded in decaying resonances. The first problem, involving direct scattering, is solved using the wave packet method. The second problem is solved by extrapolating the TD wave function using resonance eigenvalues and eigenvectors computed using a Lanczos procedure, in which $\Psi(T)$ — available from the preceding wave packet propagation — is used as starting vector, guiding Lanczos to quicker convergence.

Comparing the performance of the hybrid method with that of long-time wave packet propagation, we find that in the hybrid method the number of Hamiltonian operations required for obtaining converged reaction probabilities can be largely reduced. A reduction factor of 24 was achieved for a ''small'' two-dimensional (2D) system, in which the basis set is of size 5760. For a ''moderately large'' 4D system, a factor of 6 was achieved, the basis set size being 282 240. In both cases, the widths of the resonances — 6 for the 2D problem, 27 for 4D — are in the range 0.15–5 meV.

We conclude that the hybrid Lanczos method can be an efficient method for solving small and moderately large scattering problems affected by resonances, at least if the number of resonances affecting the scattering (approximately 30 in the present case) is not too large. In our opinion, future research should now first be directed at comparing the efficiency of the Lanczos method for extrapolation with that of rival methods, such as filter diagonalization. If the Lanczos method turns out to be also of comparable efficiency for moderately large problems, this would warrant further research directed at fine-tuning the method and extending it to very large problems. For instance, one would want to have a good *a priori* estimate for the most efficient choice of the parameter T, a point not addressed in the present work. Finally, our experience with the 4D problem indicates a need to speed up the diagonalization of complex symmetric tridiagonal matrices, if the Lanczos extrapolation method is to be extended to very large problems.

ACKNOWLEDGMENTS

We are grateful to J. K. Cullum, N. Moiseyev, N. Rom, and G. C. Groenenboom for useful suggestions and discussions. We also thank M. R. Wall and J. W. Pang for useful discussions. This research was made possible through a grant of computer time by the Dutch National Computing Facilities foundation (NCF), and through financial support by the Royal Netherlands Academy of Arts and Sciences (KNAW), for G. J. Kroes. D. Neuhauser is a Sloan Fellow (1996–1998) and is supported by an NSF Grant No. CHE93-14320, by an NSF Early Career Award, and by a grant from the Petroleum Research Fund.

[1] M. D. Feit, J. A. Fleck, Jr., and A. Steiger, J. Comput. Phys. **47**, 412 (1982).
[2] D. Kosloff and R. Kosloff, J. Comput. Phys. **52**, 35 (1983).
[3] H. Tal-Ezer and R. Kosloff, J. Chem. Phys. **81**, 3967 (1984).
[4] T. J. Park and J. C. Light, J. Chem. Phys. **85**, 5870 (1986).
[5] D. Neuhauser, J. Chem. Phys. **95**, 4927 (1991).
[6] D. Neuhauser and M. Baer, J. Phys. Chem. **93**, 2872 (1989).
[7] D. Neuhauser and M. Baer, J. Chem. Phys. **91**, 4651 (1989).
[8] H. F. Bowen, D. J. Kouri, R. C. Mowrey, A. T. Yinnon, and R. B. Gerber, J. Chem. Phys. **99**, 704 (1993).
[9] D. Neuhauser, R. S. Judson, D. J. Kouri, D. E. Adelman, N. E. Shafer, D. A. V. Kliner, and R. N. Zare, Science **257**, 519 (1992).
[10] D. Neuhauser, J. Chem. Phys. **100**, 9272 (1994).
[11] D. H. Zhang and J. Z. H. Zhang, J. Chem. Phys. **101**, 1146 (1994).
[12] D. G. Truhlar and A. Kuppermann, J. Chem. Phys. **52**, 3841 (1970)
[13] R. D. Levine and S. F. Wu, Chem. Phys. Lett. **11**, 557 (1971).
[14] D. G. Truhlar, Ed., *Resonances in Electron-Molecule Scattering, van der Waals complexes, and Reactive Chemical Dynamics* (American Chemical Society, Washington, D.C., 1984).
[15] G. J. Kroes and D. Neuhauser, J. Chem. Phys. (in press).
[16] V. A. Mandelshtam and H. S. Taylor, J. Chem. Phys. **102**, 7390 (1995).
[17] D. Neuhauser, J. Chem. Phys. **100**, 5076 (1994).
[18] M. R. Wall and D. Neuhauser, J. Chem. Phys. **102**, 8011 (1995).
[19] J. W. Pang and D. Neuhauser, Chem. Phys. Lett. **252**, 173 (1996).
[20] W. Zhu, Y. Huang, D. J. Kouri, C. Chandler, and D. K. Hoffman, Chem. Phys. Lett. **217**, 73 (1994).
[21] Y. Wang, T. Carrington, Jr., and G. C. Corey, Chem. Phys. Lett. **228**, 144 (1994).
[22] K. Takatsuka and N. Hashimoto, J. Chem. Phys. **103**, 6057 (1995).
[23] T. P. Grozdanov, V. A. Mandelshtam, and H. S. Taylor, J. Chem. Phys. **103**, 7990 (1995).
[24] V. A. Mandelshtam, T. P. Grozdanov, and H. S. Taylor, J. Chem. Phys. **103**, 10074 (1995).
[25] B. Liu, J. Chem. Phys. **58**, 1925 (1973); P. Siegbahn and B. Liu, *ibid*. **68**, 2457 (1978); D. G. Truhlar and C. J. Horowitz, *ibid*. **68**, 2466 (1978); **71**, 1514(E) (1979); B. R. Johnson, *ibid*. **74**, 754 (1981).
[26] C. Lanczos, J. Res. Natl. Bur. Stand. **45**, 255 (1950).
[27] H. Kono, Chem. Phys. Lett. **214**, 137 (1993).
[28] S. K. Gray, J. Chem. Phys. **96**, 6543 (1992).
[29] K. F. Milfeld and N. Moiseyev, Chem. Phys. Lett. **130**, 145 (1986).
[30] C. Iung and C. Leforestier, J. Chem. Phys. **90**, 3198 (1989).
[31] R. A. Friesner, J. A. Bentley, M. Menou, and C. Leforestier, J. Chem. Phys. **99**, 324 (1993).
[32] P.-N. Roy and T. Carrington, Jr., J. Chem. Phys. **103**, 5600 (1995).
[33] T. Ericsson and A. Ruhe, Math. Comp. **35**, 1251 (1980).
[34] F. Webster, P. J. Rossky, and R. A. Friesner, Comp. Phys. Comm. **63**, 494 (1991).
[35] S. Dallwig, N. Fahrer, C. Schlier, Chem. Phys. Lett. **191**, 69 (1992).
[36] C. Leforestier, K. Yamashita, and N. Moiseyev, J. Chem. Phys. **103**, 8468 (1995).
[37] R. E. Wyatt, Adv. Chem. Phys. **73**, 231 (1989).
[38] R. W. Freund, SIAM J. Sci. Stat. Comput. **13**, 425 (1992).
[39] H. O. Karlsson, J. Chem. Phys. **103**, 4914 (1995).
[40] G. C. Groenenboom and D. T. Colbert, J. Chem. Phys. **99**, 9681 (1993).
[41] G. Wiesenekker, G. J. Kroes, and E. J. Baerends, J. Chem. Phys. **104**, 7344 (1996).
[42] G. J. Kroes, G. Wiesenekker, E. J. Baerends, and R. C. Mowrey, Phys. Rev. B **53**, 10397, 1996.
[43] G. G. Balint-Kurti, R. N. Dixon, and C. C. Marston, J. Chem. Soc. Faraday Trans. **86**, 1741 (1990); Int. Rev. Phys. Chem. **11**, 317 (1992).
[44] R. C. Mowrey and G. J. Kroes, J. Chem. Phys. **103**, 1216 (1995).
[45] D. Neuhauser, J. Chem. Phys. **93**, 7836 (1990).
[46] D. Neuhauser, M. Baer, R. S. Judson, and D. J. Kouri, Chem. Phys. Lett. **169**, 372 (1990).
[47] J. K. Cullum and R. A. Willoughby, *Lanczos Algorithms for Large Symmetric Eigenvalue Computations, Vol. I* (Birkhäuser, Stuttgart, 1985).

[48] N. Moiseyev, P. R. Certain, and F. Weinhold, Mol. Phys. **36**, 1613 (1978).
[49] N. Moiseyev, *Lecture Notes in Physics* (Springer-Verlag: New York, 1984), Vol. 211, p. 235.
[50] W. P. Reinhardt, Annu. Rev. Phys. Chem. **33**, 223 (1982).
[51] N. Moiseyev, Isr. J. Chem. **31**, 311 (1991).
[52] O. Kolin, C. Leforestier, and N. Moiseyev, J. Chem. Phys. **89**, 6836 (1988).
[53] G. J. Kroes, J. G. Snijders, and R. C. Mowrey, J. Chem. Phys. **102**, 5512 (1995).
[54] G. J. Kroes, J. G. Snijders, and R. C. Mowrey, J. Chem. Phys. **103**, 5121 (1995).
[55] G. Jolicard and E. J. Austin, Chem. Phys. **103**, 295 (1986).
[56] M. Garcia-Sucre and R. Lefebvre, J. Chem. Phys. **85**, 4753 (1986).
[57] N. Rom, N. Lipkin, and N. Moiseyev, Chem. Phys. **151**, 199 (1991).
[58] U. V. Riss and H.-D. Meyer, J. Phys. B **26**, 4503 (1993).
[59] Á. Vibók and G. G. Balint-Kurti, J. Phys. Chem. **96**, 8712 (1992).
[60] R. N. Bracewell, *The Fourier Transform and its Applications* (McGraw-Hill, New York, 1986).
[61] W. H. Press, S. A. Teukolsky, W. T. Vetterling, and B. P. Flannery, *Numerical Recipes in FORTRAN*, 2nd ed. (Cambridge University Press, Cambridge, 1992).
[62] J. K. Cullum and R. A. Willoughby, *Lanczos Algorithms for Large Symmetric Eigenvalue Computations*, Vol. II (Birkhäuser, Stuttgart, 1985).
[63] R. Kosloff, J. Phys. Chem. **92**, 2087 (1988).
[64] Y. Huang, W. Zhu, D. J. Kouri, and D. K. Hoffman, Chem. Phys. Lett. **206**, 96 (1993); (E) **213**, 209 (1993).
[65] V. A. Mandelshtam and H. S. Taylor, J. Chem. Phys. **103**, 2903 (1995).
[66] G. J. Kroes, G. W. Wiesenekker, E. J. Baerends, R. C. Mowrey, and D. Neuhauser, J. Chem. Phys. (in press).